RESEARCH PAPERS

Acta Cryst. (1998). B**54**, 351–357

β-$Al_{4.5}FeSi$: A Combined Synchrotron Powder Diffraction, Electron Diffraction, High-Resolution Electron Microscopy and Single-Crystal X-ray Diffraction Study of a Faulted Structure

V. Hansen,[a] B. Hauback,[b] M. Sundberg,[c] Chr. Rømming[d] and J. Gjønnes[a]*

[a]*Center for Materials Science, University of Oslo, Gaustadalleen 21, N-0371 Oslo, Norway,* [b]*Institute for Energy Technology, N-2007 Kjeller, Norway,* [c]*Department of Inorganic Chemistry, Arrhenius Laboratory, Stockholm University, S-10691 Stockholm, Sweden, and* [d]*Department of Chemistry, University of Oslo, PO Box 1033 Blindern, N-0315 Oslo, Norway. E-mail: jon.gjonnes@fys.uio.no*

(*Received 24 July 1997; accepted 17 November 1997*)

Abstract

A previous single-crystal X-ray and electron diffraction structure study [Rømming *et al.* (1994). *Acta Cryst.* B**50**, 307–312] of the heavily faulted alloy phase β-$Al_{4.5}FeSi$ has been extended by synchrotron powder data and further electron microscopy and diffraction observations. Reflections that were omitted in the single-crystal work could be included in the powder refinement, which resulted in some adjustment of cell parameters and atom coordinates. The double *c* axis reported by some authors is explained by periodic faults in the structure, which is described in terms of a tetragonal sub-unit. Apparent discrepancies between refinement from single-crystal and powder data are discussed briefly.

1. Introduction

Structure determination of crystalline phases with a high density of faults can offer complications, even for relatively small unit-cell sizes. An example is the intermetallic phase β-$Al_{4.5}FeSi$, which occurs commonly as primary particles in industrial aluminium alloys. The phase has already been identified in the ternary Al–Fe–Si system by Rosenhain *et al.* (1921); attempts to solve the crystal structure can be found in the literature, *e.g* Black (1954). Only recently has a successful structure determination been carried out, by a combined single-crystal X-ray and electron diffraction study by three of us (Rømming *et al.*, 1994). The main problem was associated with prolific faults, which severely influenced some of the single-crystal X-ray intensities. This difficulty could be overcome with the aid of a detailed electron diffraction survey throughout the reciprocal space. In this way the space group *A*2/*a* could be determined and the reflections which are most strongly affected by faults were sorted out. Of 980 unique reflections measured by X-ray diffractometry, 244 reflections with $h + k + l = 2n + 1$ were weak and disturbed by diffuse streaks; these were omitted from the structure determination. The resulting monoclinic average structure (*A*2/*a*; $a = 6.161$, $b = 6.175$, $c = 20.81$ Å, $\beta = 90.42°$) was refined to a conventional *R* value of 0.039. A representation of the *A*-centred sub-unit of the structure by coordination polyhedra is shown in Fig. 1.

Although successful and chemically satisfactory, this structure determination left some unsolved problems: a quarter of the reflections had been omitted because of faults; silicon was not located; the faults were not specified. In the literature the unit cell is sometimes quoted with a double *c* axis and with β angles varying from 90 (orthorhombic or tetragonal) to 91° (Phragmèn, 1950; Black, 1954; Høier *et al.*, 1977; Carpenter & Le Page, 1993). Therefore, it was decided to supplement our previous structure study with synchrotron powder diffraction from the same material. The powder refinement deviated significantly from the previous single-crystal X-ray result in some respects; the most notable differences were the β angle of 91.0°, which is appreciably different from the single-crystal value of 90.4°, and

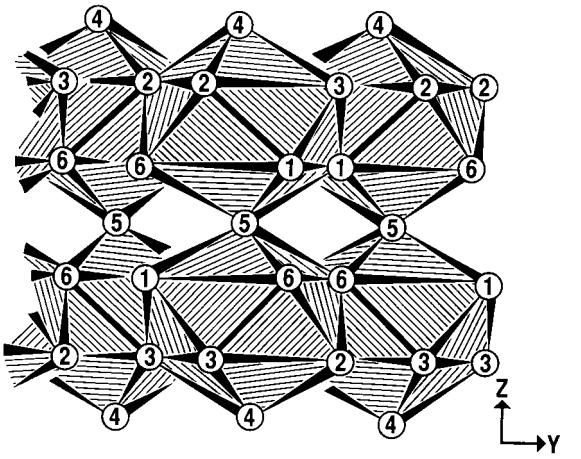

Fig. 1. Half of the *a*-centred unit cell of β-$Al_{4.5}FeSi$ represented by two double layers of double-capped square antiprisms.

some broad extra lines. In the present paper these observations together with further electron diffraction and microscopy results are reported and interpreted in terms of faults and superstructures, which can be described in terms of a basic tetragonal unit with $c_t = c/2$. The published structure (Rømming *et al.*, 1994) is thus seen as a monoclinic average structure with the c axis, whereas the unit cells reported in the literature with the double c axis $2c$ should be regarded as superstructures.

2. Experimental

The preparation of β-$Al_{4.5}FeSi$ crystals from a melt by a careful cooling procedure, followed by electrolytical dissolution, and selection of the best fragments for single-crystal work was described in the previous article (Rømming *et al.*, 1994). In that paper the technical details of electron diffraction and microscopy investigations in the Jeol 200CX and Jeol 2000FX were also given. In addition, we have used a Jeol 3010 microscope (URP31 pole-piece, double-tilt side-entry stage) at 300 kV for high-resolution imaging.

Powder X-ray diffraction data were collected on the two-circle diffractometer at the Swiss–Norwegian beamline (SNBL) at the European Synchrotron Radiation Facility (ESRF), Grenoble. The sample, obtained from the same material as above, was held in a rotating boron–silicate glass capillary of diameter 0.5 mm. X-rays of wavelength 1.0983 Å were obtained from a channel-cut Si(111) monchromator; the wavelength was calibrated with a Si powder standard. Intensity data were collected in the angular range 5–82° in 2θ using a step length of 0.010°, see Fig. 2(*a*).†

Table 1. *Cell parameters from single-crystal X-ray (X) and synchrotron powder data (S)*

	a	*b*	*c*	β
X	6.161 (3)	6.175 (3)	20.813 (6)	90.42 (3)
S	6.1676 (1)	6.1661 (1)	20.8093 (3)	91.00 (1)

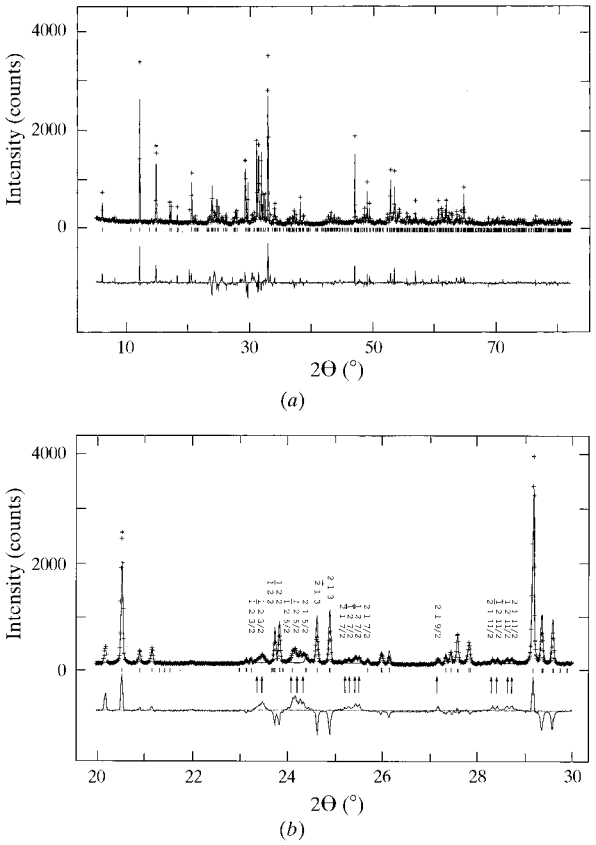

Fig. 2. (*a*) Synchrotron powder pattern of β-$Al_{4.5}FeSi$; experimental data indicated by crosses; fitted curve as a continous line, with β reflection positions and difference curve shown below. (*b*) Part of the pattern in (*a*) with reflections $12l$ and $21l$, $l = n + 1/2$, as well as superstructure reflections ($l = n + 1/2$), are marked by arrows; note also negative differences for the β reflections with $l = n$.

3. Powder diffraction

Structural and instrumental parameters for the powder data were obtained from a Rietveld-type refinement using the *GSAS* program system (Larson & Von Dreele, 1994). Atomic scattering factors were taken from the *GSAS* library. Peak shapes were described by the pseudo-Voigt function. The background was simulated using a cosine Fourier series polynomial. Unit-cell parameters and atomic coordinates from the single-crystal X-ray refinements (Rømming *et al.*, 1994) were entered as starting points for the Rietveld refinements. The β angle differed significantly, *viz.* 90.42 (3) and 91.00 (1)°, for the single-crystal and powder refinements, respectively, see discussion below. Only small differences were found for the the other cell parameters and minor shifts in the atomic coordinates between the two refinements, see Tables 1 and 2. Examination of the peaks in the powder diffraction pattern revealed additional reflections not accounted for by the single-crystal structure model. Fig. 2(*b*) shows part of the pattern with additional peaks marked by arrows. These lines could not be related to other phases in the system and are found in a region where diffuse lines and extra spots appear in electron diffraction patterns, see below. Owing to the additional peaks that were not included in the structure model, $R_p = 0.121$ and $R(F^2) = 0.162$ were considered to be satisfactory.

† The numbered intensity of each measured point on the profile has been deposited with the IUCr (Reference: AB0388). Copies may be obtained through The Managing Editor, International Union of Crystallography, 5 Abbey Square, Chester CH1 2HU, England. The powder pattern has also been deposited with the ICDD as PDF no. 49-1.

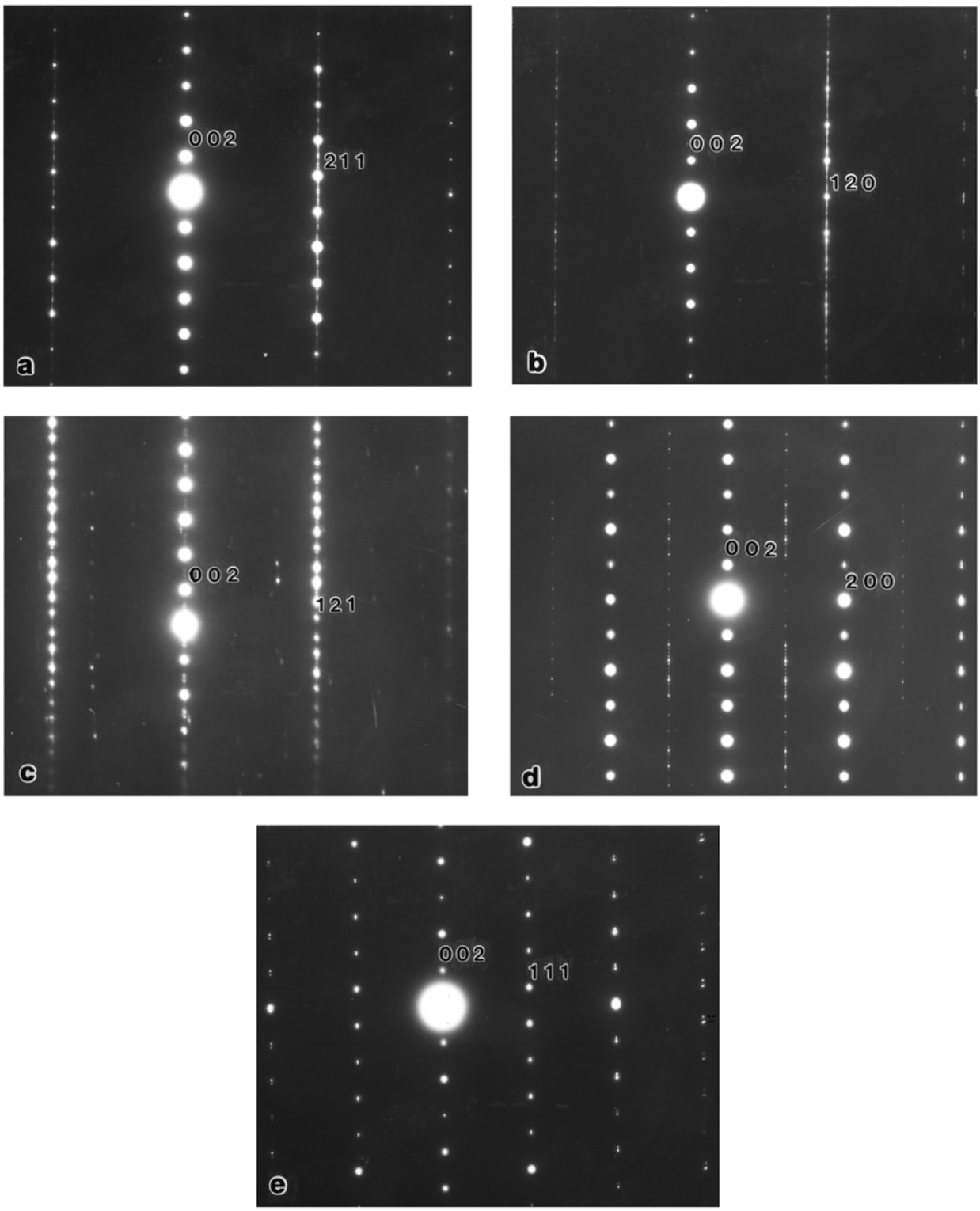

Fig. 3. Selected-area electron diffraction patterns along directions (*a*) [$\bar{1}\bar{2}0$], (*b*) and (*c*) [$\bar{2}10$], (*d*) [010] and (*e*) [110] with streaks and superstructure spots along rows with $h + k = 2n + 1$. Note the absence of β reflections along the $12l$ row of (*d*), where only $l = n + 1/2$ reflections are seen.

4. Electron diffraction and microscsopy

Electron diffraction patterns taken in the previous study (Rømming *et al.*, 1994) were supplemented by concentrating on the diffuse streaks and superstructure spots. The patterns shown in Figs. 3(*a*)–(*d*), with beam directions [010], [110], [$\bar{1}$20] and [$\bar{2}$10], show streaks running in the c^* direction, through spots with $h + k = 2n + 1$. The most prominent streaks appear along 12l rows, where superlattice spots are often seen for $l = n + 1/2$; sometimes the reflections from the average c lattice ($l = 2n$) are absent on these rows, with only superlattice reflections remaining, Fig. 3(*d*). Streaks and extra spots are somewhat less frequent along the rows with $h = 2n$, $k = 2n + 1$, *e.g.* 21l. Along rows with $h + k = 2n$ only faint streaking and extra spots, which may be attributed to double scattering, are seen. Note that streaks and superstructure spots also appear along 10l, where all reflections would be expected to be absent due to the a glide. Splitting due to twinning is seen in projections that do not include b^*, *e.g.* [010] and [1$\bar{1}$0] projections, Figs. 3(*d*) and (*e*). The β angle could be estimated from the split; the angle obtained from [010] patterns appeared to be smaller and with larger variations than the value estimated from [1$\bar{1}$0] projections: $\beta_{[010]} = 90.7 \pm 0.2$; $\beta_{[1\bar{1}0]} = 91.0 \pm 0.1^\circ$. Twinned regions are shown in the dark-field micrograph in Fig. 4. The near-tetragonal character of the structure is apparent from the convergent-beam pattern, Fig. 5.

High-resolution electron micrographs taken in the [2$\bar{1}$0] projection reveal many faults on (001), frequently with a double period. The contrast variation associated with the periodic faults is quite weak in thin regions, Fig. 6(*a*), but becomes more pronounced in thicker regions, Fig. 6(*b*), where a mixture of double and single periods is seen.

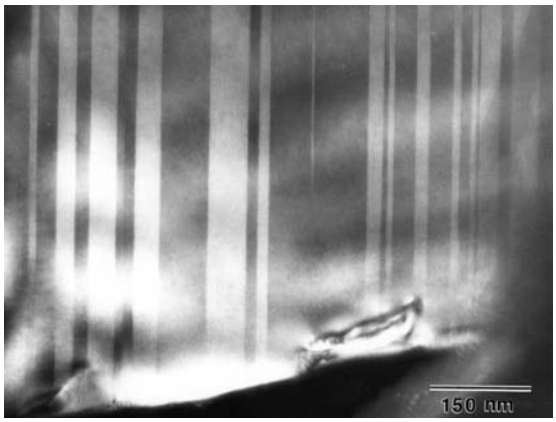

Fig. 4. Dark field micrograph taken with a diffuse streak with superstructure spots.

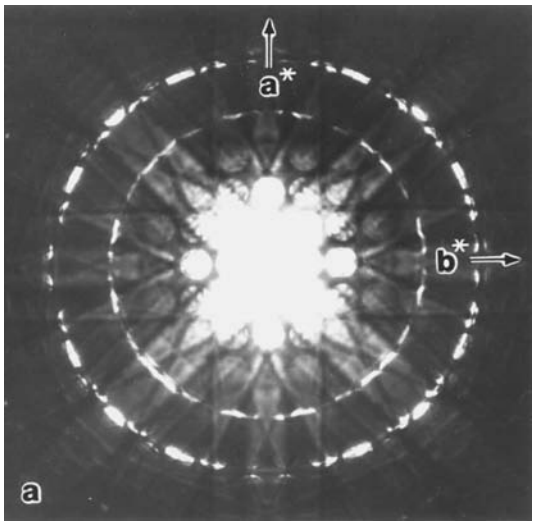

Fig. 5. CBED pattern taken around [001] shows almost 4m symmetry.

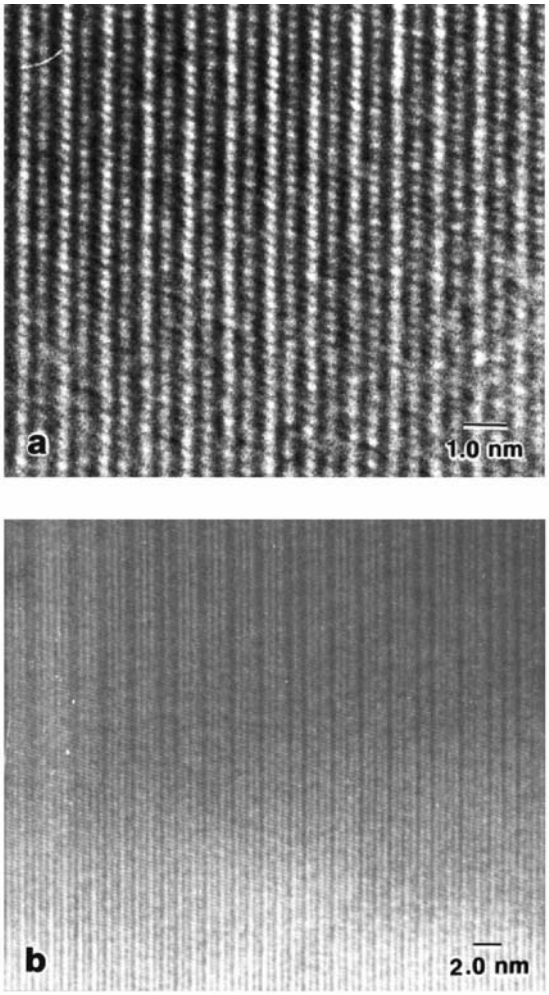

Fig. 6. High-resolution images taken along [2$\bar{1}$0], from thin and thick regions, respectively.

Table 2. *Coordinates from single-crystal X-ray (X), synchrotron powder (S) and tetragonally adjusted (T) refinements*

x, *y* and *z* refer to the β-$Al_{4.5}FeSi$ unit cell; *x*′, *y*′ and *z*′ refer to an origin shifted to the pseudo-tetragonal axis, see Fig. 7. For the sake of comparison with the tetragonal sub-unit (T), some of the atoms [Al(1), Al(6) and Al(2), Al(3)] are given by other equivalent positions than those listed by Rømming *et al.* (1994).

	x	*x*′	*y*	*y*′	*z*	*z*′
Fe (X)	0.5024 (1)	0.0024	0.2605 (5)	0.0105	0.1367 (3)	−0.1133
(S)	0.5030 (4)	0.0030	0.2477 (4)	−0.0023	0.1366 (1)	−0.1134
Fe (T)		0		0		−0.113
Al(1) (X)	0.8583 (3)	0.3583	0.3938 (3)	0.1438	0.1863 (1)	−0.0637
(S)	0.8608 (9)	0.3608	0.3920 (10)	0.1420	0.1871 (3)	−0.0630
Al(6) (X)	0.8574 (3)	0.3574	0.4000 (3)	0.1500	0.3164 (1)	0.0664
(S)	0.8497 (9)	0.3497	0.4033 (10)	0.1533	0.3165 (3)	0.0665
Al(1,6) (T)		0.356		0.144		−0.065
Al(2) (X)	0.6613 (3)	0.1613	0.5884 (3)	0.3384	0.4103 (1)	0.1603
(S)	0.6657 (9)	0.1657	0.5843 (10)	0.3343	0.4084 (3)	0.1584
Al(2,3) (T)		0.165		0.335		0.158
Al(3) (X)	0.6669 (3)	0.1669	0.5833 (3)	0.3333	0.0908 (1)	−0.1592
(S)	0.6691 (9)	0.1691	0.5791 (10)	0.3291	0.0939 (3)	−0.1561
Al(4) (X)	0.4972 (3)	−0.0028	0.2666 (7)	0.0166	0.0181 (1)	−0.2419
(S)	0.4921 (7)	−0.0079	0.2490 (12)	−0.0010	0.0189 (2)	−0.2411
Al(4) (T)	(4)	0		0		−0.241
Al(5) (X)	1/2	0	1/4	0	1/4	0
(S)	1/2	0	1/4	0	1/4	0
Al(5)(T)		0		0		0

5. Discussion – a fault model

The unit-cell dimensions of β-$Al_{4.5}FeSi$ are close to those of a tetragonal cell. Diffraction patterns, *e.g.* electron diffraction spot patterns or CBED (convergent-beam electron diffraction patterns) taken near the [001] axis (Fig. 5), indicate an almost tetragonal 4*m* symmetry, as was in fact proposed by Black (1954) from X-ray Laue photographs. The tetragonal character of the structure reported by Rømming *et al.* (1994) is most clearly seen by considering half the unit cell as a tetragonal subcell

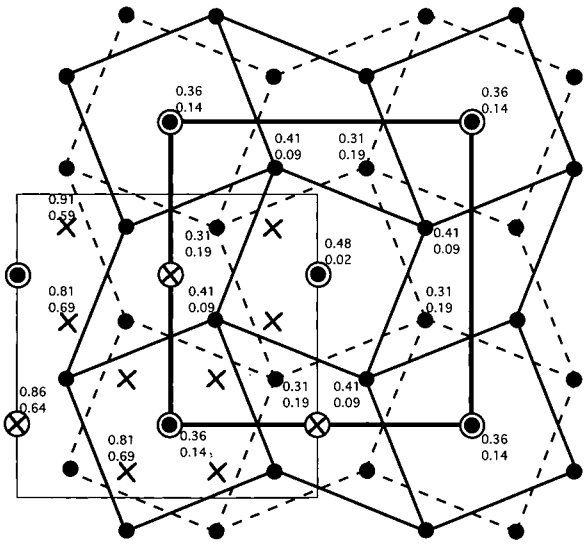

Fig. 7. Projected β-$Al_{4.5}FeSi$ structure along *c**. Atoms in the upper half of the cell are marked with crosses. The tetragonal sub-cell with its origin at $x = \frac{1}{2}$, $y = \frac{1}{4}$ is indicated; this cell includes only atoms in the lower half of β.

with $a = b = 6.16$, $c = 10.4$ Å, which corresponds to the translational unit, see Fig. 7, where the origin is shifted so as to coincide with the 'pseudo-fourfold axis', see the list of coordinates in Table 2. The β structure can then be described formally as a periodic antiphase structure based on the translation unit, with the displacement vector **b**/2 at every (002) plane,† and a slight monoclinic distortion.

Another displacement, **a**/2, is also possible; this will result in the same structure, but with the monoclinic axis along **a**. A combination of the two will lead to faults. In this picture we can describe the monoclinic structure β-$Al_{4.5}FeSi$ by a sequence of displacements **b**/2

$$\ldots//\frac{\mathbf{b}}{2}//\frac{\mathbf{b}}{2}//\frac{\mathbf{b}}{2}//\ldots.$$

A fault in β can be written as

$$\ldots//\frac{\mathbf{b}}{2}//\frac{\mathbf{b}}{2}//\frac{\mathbf{a}}{2}//\frac{\mathbf{b}}{2}//\frac{\mathbf{b}}{2}//\ldots$$

and a superstructure with a double *c* axis

$$\ldots//\frac{\mathbf{b}}{2}//\frac{\mathbf{a}}{2}//\frac{\mathbf{b}}{2}//\frac{\mathbf{a}}{2}\ldots,$$

see Fig. 8. Further possibilities arise when we take into account that the monoclinic deformation can have two directions, which may be denoted **b**/2 and $\bar{\mathbf{b}}$/2. A twin may be represented by

$$\ldots//\frac{\mathbf{b}}{2}//\frac{\mathbf{b}}{2}//\frac{\bar{\mathbf{b}}}{2}//\frac{\bar{\mathbf{b}}}{2}\ldots.$$

Many combinations of faults and twins are possible, as is indeed indicated by the variations seen in electron

† Indexing here and in the following is in terms of the β-$Al_{4.5}FeSi$ cell.

diffraction spot patterns. The simplest fault model may be the superstructure with a double c axis indicated by the sequence above, see Fig. 8(b). This structure can be described as an antiphase structure with a displacement vector $[\frac{1}{2}\ \frac{1}{2}\ 0]$ on every (001) plane of β. Some patterns can be indexed according to this cell, with the superstructure reflections for $l = n + 1/2$ along rows with $h + k = 2n + 1$. An expression for the amplitude of scattering can be written in terms of the translation unit of β or in terms of F^{β}

$$F^{2c}_{hkl} = F^{\beta}_{hkl}\{1 + \exp[\pi i(h + k + 2l)]\},$$

which will produce extra reflections along the $h + k = 2n + 1$ row; along these rows the β cell reflections will be missing. In most cases the superstructure appears together with β, but occasionally one finds pure superstructure regions, as in Fig. 3(d). The extra reflections are most clearly seen along [12l] and, less frequently, along [21l] in electron diffraction patterns. In the powder pattern both 12l and 21l reflections are seen with $l = n + 1/2$, whereas the reflections with $l = n$ are significantly lower than the calculated result for the β structure.

The fault model also offers an explanation for other apparent discrepancies between the synchrotron powder and single-crystal X-ray results, in particular, the β angle. The X-ray data were obtained as an average over a crystal which contained faults (even if care was taken

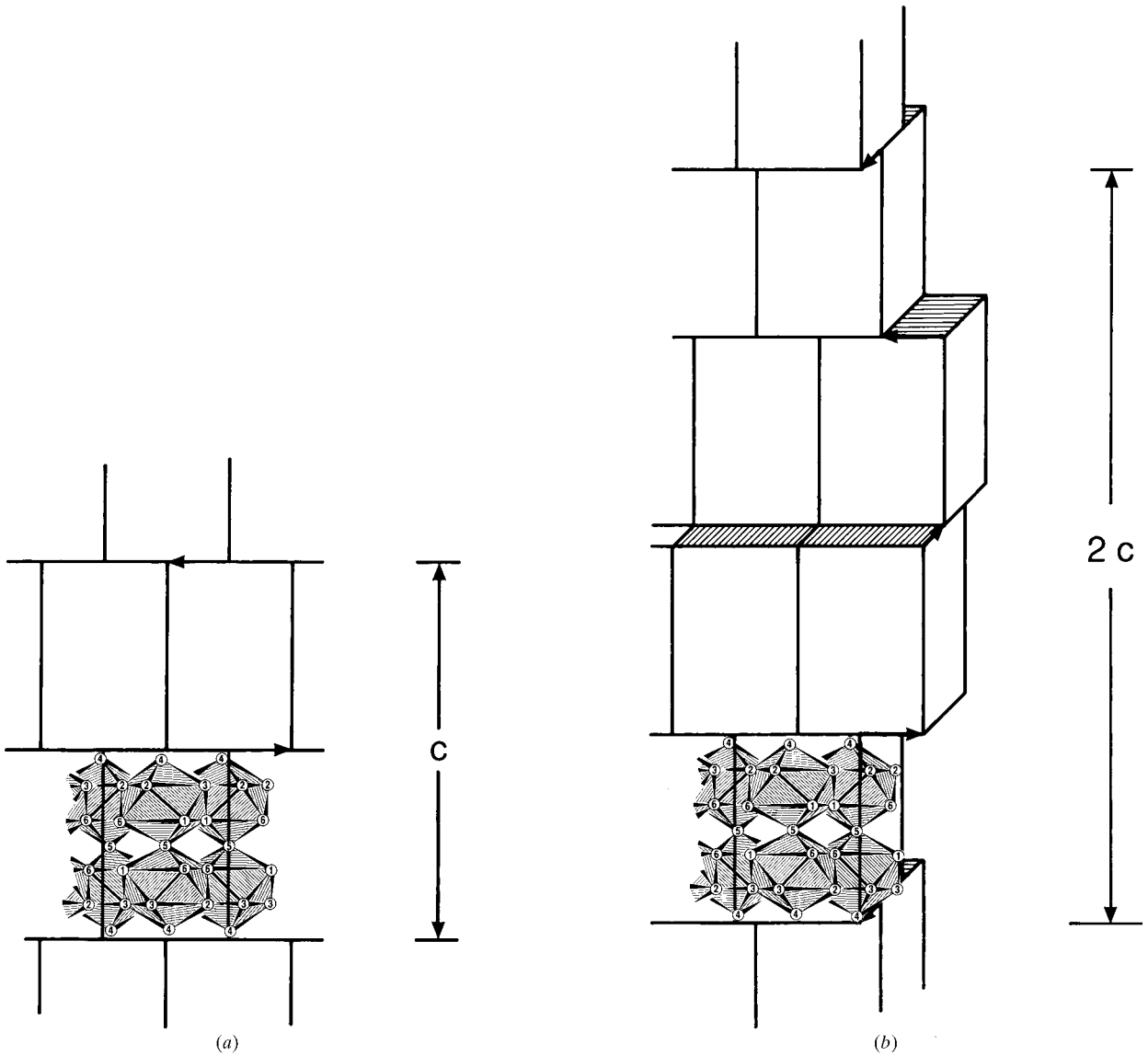

Fig. 8. (a) Schematic representation of β-$Al_{4.5}FeSi$ structure; the shifts $\pm\mathbf{b}/2$ are indicated. (b) Schematic representation of the 2(c) superstructure; the shifts $\pm\mathbf{b}/2$ and $\pm\mathbf{a}/2$ are indicated.

to select the 'best' fragment). **a**/2 faults are expected to reduce the β angle, by tilting the c axis towards **b** rather than **a**. Also note that the angle seen in the $[1\bar{1}0]$ direction would be less affected by this type of fault, as seems to be reflected in the estimates of β quoted above from $[1\bar{1}0]$ and [010] electron diffraction patterns, respectively.

The main deviation in coordinates appears in the positions of Fe and Al(4). These are the atoms near the 'pseudo-four fold axis'. For these atoms the powder refinement yielded values much closer to the pseudo-axis. Tentatively, we may attribute this to the omission of reflections with $h + k = 2n + 1$ in the single-crystal refinement, when these in principle could take any value. The powder refinement includes the fact that these are generally weak; we may therefore expect that the powder result is more correct in that respect.

The superstructure with a double c axis offers an explanation for the previous reports of a unit cell with the c axis in the range 41–42 Å. However, the observed reflections may indicate that a space group cannot be readily assigned; it is best described as an anti-phase structure based on the ideal β structure reported by Rømming *et al.* (1994). From this discussion it may be expected that the anti-phase structure will destroy the monoclinic symmetry and in fact become triclinic.

Financial support from the Norwegian Research Council is gratefully acknowledged.

References

Black, P. J. (1954). *Philos. Mag.* **46**, 401–409.
Carpenter, G. J. C. & Le Page, Y. (1993). *Scr. Metall. Mater.* **28**, 733–736.
Høier, R., Lohne, O. & Mørtvedt, S. (1977). *Scand. J. Metall.* **6**, 36–37.
Larson, A. C. & Von Dreele, R. B. (1994). *GSAS. General Structure Analysis System*. MS-H805, Los Alamos National Laboratory, Los Alamos, New Mexico, USA.
Phragmèn, G. (1950) *J. Inst. Met.* **77** 489–552.
Rømming, Chr., Hansen, V. & Gjønnes, J. (1994). *Acta Cryst.* B**50**, 307–312.
Rosenhain, W., Archbutt, S. L. & Hanson, D. (1921). Eleventh Report to the Alloys Research Committee of the Institute of Mechanical Engineers, pp. 211–212.